UNIVERSITY *of York*

This is a repository copy of *Magnetic domain-wall creep driven by field and current in Ta/CoFeB/MgO*.

White Rose
university consortium
Universities of Leeds, Sheffield & York

Magnetic domain-wall creep driven by field and current in Ta/CoFeB/MgO

S. DuttaGupta, S. Fukami, B. Kuerbanjiang, H. Sato, F. Matsukura, V. K. Lazarov, and H. Ohno

---

Articles you may be interested in

Electrical switching of antiferromagnets via strongly spin-orbit coupled materials
AIP Advances **121**, 023907023907 (2017); 10.1063/1.4974027

Robust spin-current injection in lateral spin valves with two-terminal Co2FeSi spin injectors
AIP Advances **7**, 055808055808 (2016); 10.1063/1.4972852

Electric-current-induced dynamics of bubble domains in a ferrimagnetic Tb/Co multilayer wire below and above the magnetic compensation point
AIP Advances **7**, 055916055916 (2017); 10.1063/1.4974067

Enhancement of voltage-controlled magnetic anisotropy through precise control of Mg insertion thickness at CoFeB|MgO interface
AIP Advances **110**, 052401052401 (2017); 10.1063/1.4975160

Magnetic domain-wall creep driven by field and current in Ta/CoFeB/MgO

S. DuttaGupta,[1,2] S. Fukami,[1,2,3,4,a] B. Kuerbanjiang,[5] H. Sato,[2,3,4] F. Matsukura,[1,2,3,6] V. K. Lazarov,[5] and H. Ohno[1,2,3,4,6]

[1]*Laboratory for Nanoelectronics and Spintronics, Research Institute of Electrical Communication, Tohoku University, 2-1-1 Katahira, Aoba-ku, Sendai 980-8577, Japan*
[2]*Center for Spintronics Research Network, Tohoku University, 2-1-1 Katahira, Aoba-ku, Sendai 980-8577, Japan*
[3]*Center for Spintronics Integrated Systems, Tohoku University, 2-1-1 Katahira, Aoba-ku, Sendai 980-8577, Japan*
[4]*Center for Innovative Integrated Electronic Systems, Tohoku University, 468-1 Aramaki Aza Aoba, Aoba-ku, Sendai 980-0845, Japan*
[5]*Department of Physics, University of York, Heslington, York YO10 5DD, United Kingdom*
[6]*WPI-Advanced Institute for Materials Research, Tohoku University, 2-1-1 Katahira, Aoba-ku, Sendai 980-8577, Japan*

Creep motion of magnetic domain wall (DW), thermally activated DW dynamics under subthreshold driving forces, is a paradigm to understand the interaction between driven interfaces and applied external forces. Previous investigation has shown that DW in a metallic system interacts differently with current and magnetic field, manifesting itself as different universality classes for the creep motion. In this article, we first review the experimental determination of the universality classes for current- and field-driven DW creeps in a Ta/CoFeB/MgO wire, and then elucidate the underlying factors governing the obtained results. We show that the nature of torque arising from current in association with DW configuration determines universality class for the current-induced creep in this system. We also discuss the correlation between the field-induced DW creep characteristics and structure observed by a transmission electron microscope. The observed results are expected to provide a deeper understanding for physics of DW motion in various magnetic materials. *© 2017 Author(s). All article content, except where otherwise noted, is licensed under a Creative Commons Attribution (CC BY) license (http://creativecommons.org/licenses/by/4.0/).* [http://dx.doi.org/10.1063/1.4974889]

I. INTRODUCTION

Dynamical behavior of elastic interfaces under the application of forces is a challenging problem in a multitude of physical systems from different branches of science.[1–4] In this context, magnetic domain wall (DW) motion under the action of forces (current and/or magnetic field) is a prototypical example for an elastic interface in this field of interest. The application of forces sets DW in motion and shows a variety of features depending on the magnitude of the applied force with respect to a threshold which is relevant technologically as well as of fundamental interest. For applied forces larger than the threshold, fast DW motion is induced by application of forces which is prospective for next generation spintronic devices.[5,6] On the other hand, for applied forces smaller than the threshold, DW motion occurs with the assistance of thermal activation, commonly referred to as creep motion. DW velocity (v) in the creep regime obeys a universal scaling relation with respect to the applied forces (f) as $\ln v \propto f^{-\mu}$ with a creep exponent μ representing the universality class.[7] Investigation of the

[a]Author to whom correspondence should be addressed. E-mail: s-fukami@riec.tohoku.ac.jp.

universality classes of DW creep motion under the action of current and/or magnetic field is an important subject for the identification of underlying mechanisms of DW motion, which eventually leads to better understandings of the dynamics of various elastic interfaces. The universality classes for field-induced DW creep are known to depend on the nature of the disorder; random bond (RB) or random field (RF), which manifests as $\mu = 0.25$ or 1, respectively.[4,8–11] On the other hand, universality classes for current-induced creep revealed interesting scenario. For a magnetic semiconductor (Ga,Mn)As with the RF disorder, it was shown that current-induced DW creep belongs to a different universality class characterized by $\mu = 0.33 \pm 0.06$.[8] Meanwhile, for a metallic system Pt/Co/Pt, current-induced creep belongs to the same universality class as field-induced creep with the RB disorder.[11] The same driving force (i.e., current) thus evidences dissimilar behavior for semiconducting and metallic systems, which requires further clarification. While different universality classes for current-induced creep between these two systems can be ascribed to a fundamental difference in the nature of torque induced by current, one of the pertinent questions was whether different universality classes for field- and current-induced DW creeps could be observed in metallic systems. Our previous work utilizing Ta/CoFeB/MgO system with ultrathin Ta underlayer provided solution to this disparity, where field-induced DW creep belongs to the RB class and current-induced DW creep is characterized by $\mu = 0.39 \pm 0.06$.[12] In this article, we first review our previous results for field- and current-induced DW creep, and then elucidate the factors which play a key role for determination of the universality class in the context of metallic systems. We show that nature of torque in association with DW configuration determines universality class for current-induced DW creep. Our investigations of current- and field-induced DW creeps are expected to shed light on the long-standing question of the determining factors for universality classes for DW creep. We have also performed structural characterization using transmission electron microscopy (TEM) on cross-section specimens prepared by standard methods.[13] The observed characteristics of field-driven DW motion properties are discussed in the light of the structural properties of Ta/CoFeB/MgO thin film.

II. EXPERIMENTAL PROCEDURES

The stack structure used for field (H) and current (I)-driven DW creep experiments is from the substrate side Ta (0.5 nm)/CoFeB (1.2 nm)/MgO (1.5 nm)/Ta (1 nm). We employ DC and RF magnetron sputtering for deposition of the film on a thermally oxidized Si substrate. The blanket films and μm-sized devices are subsequently annealed at 300°C for 1 hour in a magnetic field of 0.4 T along the film normal direction. Magnetization curves shown in Fig. 1(a) indicate that the stack structure possesses an out-of-plane easy axis[14] with spontaneous magnetization of 1.36 T and effective anisotropy constant of 2.82×10^5 J/m^3. H- and I-driven DW motions are investigated by a magneto-optic Kerr effect (MOKE) microscope equipped with a liquid He cryostat.

Wire shaped devices of width 5 μm and length 60 μm are patterned by photolithography and Ar ion milling, followed by the annealing. To study the temperature (T) dependence of H- and I-driven DW motion, started from a uniform magnetization state, DW is first created by passing

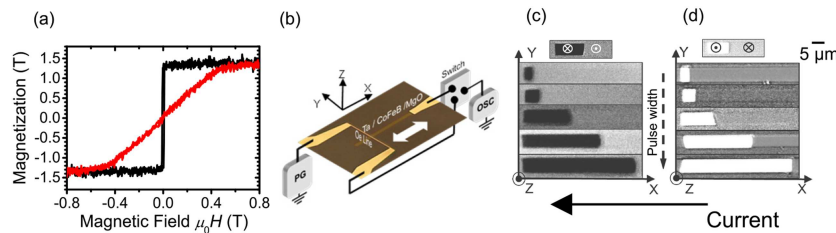FIG. 1. (a) In-plane (red) and out-of-plane (black) magnetization curves of blanket film. (b) Measurement setup for field- and current-driven DW creep measurements. (c), (d) MOKE images of DW displacement under constant current density $J = 1.5 \times 10^{11}$ A/m^2 with various pulse widths (1, 2.5, 5, 7.5, and 10 ms from top to bottom) at room temperature for down-up (c) and up-down (d) domain configurations, respectively.

current through the Oersted line placed transverse to the wire as shown in Fig. 1(b), and then moved toward the other end by applying H or I pulses. The displacement is recorded with the MOKE microscope as shown in Figs. 1(c) and (d), and v is determined from a linear fit of DW displacement vs. integrated pulse width at a constant amplitude. For I-driven experiments, stage temperature is set so that the device temperature is constant after injection of current pulses, eliminating artefacts from the Joule heating. To obtain further insights into DW creep phenomena, we study H-driven expansion of magnetic bubble domains in blanket films with identical stack structure under the application of magnetic fields (in-plane and/or out-of-plane) at room temperature. Nucleation of magnetic bubble domains succeeded by propagation are induced by H pulses sourced by a mm-sized coil placed in close proximity to the sample. For investigations concerning simultaneous application of in-plane and out-of-plane magnetic fields, out-of-plane pulses are applied under a static in-plane field.

III. FIELD- AND CURRENT-INDUCED DW CREEP IN Ta/CoFeB/MgO

We here review the previous results for H- and I-induced DW creep in a μm-sized Ta/CoFeB/MgO wire.[12] DW creep motion can be understood as the motion of an elastic interface creeping over pinning sites under application of force f (= H or I) given by the relation:[4,7–12]

$$v = v_0 \exp\left[\frac{U_C}{k_B T}\left(\frac{f_C}{f}\right)^\mu\right], \tag{1}$$

where v_0 is threshold velocity, f_C is critical force, U_C is pinning potential, and k_B is the Boltzmann constant. We investigated the H- and I-driven DW motion as a function of T. The out-of-plane field (H_Z) and current density (J) dependences of v are shown in Figs. 2(a) and (c), respectively, in which non-linear behaviour implies the motion is in creep regime. For H-driven case, fitting of the data by Eq. (1) using μ as a free variable resulted in an average value of $\mu = 0.23\pm0.07$. On the other hand, fitting using the same procedure for I-driven case resulted in $\mu = 0.39\pm0.06$. The good accordance between experimental data and fitting results as shown in the scaling plots in Figs. 2(b) and (d) proves that the observed motion can be well described by the creep model with the obtained μ. In addition, the slope of scaling curve for H-driven case enables the quantification of strength of energy barrier to DW motion through the effective critical field, commonly given as $H_C^{\text{eff}} = (U_C/k_B T)^{1/\mu} H_C$ where H_C represents the intrinsic critical field required for DW motion under no thermal agitation. The energy barrier to H-driven DW motion is a measure of DW pinning strength which is an important parameter for devices utilizing magnetization reversal governed by DW propagation. We observe that H_C^{eff} in Ta/CoFeB/MgO system shows weak temperature dependence with virtually constant magnitude $\mu_0 H_C^{\text{eff}} \simeq 10^3$ T (μ_0 is permeability). Interestingly, the value of $\mu_0 H_C^{\text{eff}}$ in Ta/CoFeB/MgO system is two to three orders of magnitude smaller than that for other metallic systems at similar device dimensions.[15,16]

The obtained value of μ for H- and I-driven creep and the related effective critical fields provide several important information concerning DW creep motion in Ta/CoFeB/MgO. μ is invariant
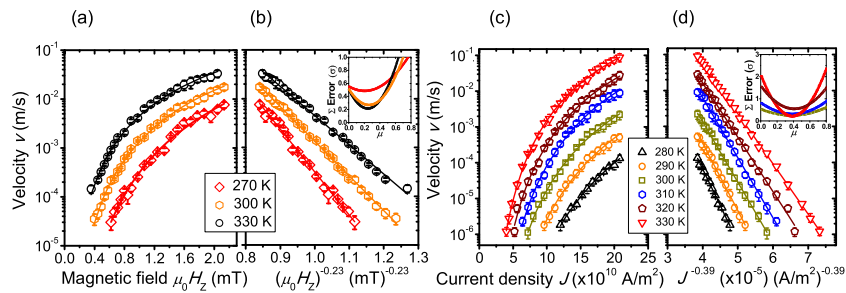

FIG. 2. (a) Temperature dependence of DW velocity v vs. magnetic field $\mu_0 H_Z$. (b) Scaling plot of log v vs. $(\mu_0 H_Z)^{-0.23}$. (c) Temperature dependence of DW velocity v vs. current density J. (d) Scaling plot of log v vs. $J^{-0.39}$. Insets of (b) and (d) are evaluation of the exponent μ from standard error curve. Solid lines indicate fitting curve with Eq. (1).

with respect to T and also to device dimensions (not shown), indicating that observed difference in universality classes should be related to the internal dynamics of motion induced by H and I. Universality class for H-driven creep motion in our system belongs to the universality class for RB disorder commonly prevalent in magnetic metals.[4,9,11] On the other hand, the obtained value of μ for I-driven creep which is incompatible with RB or RF class can be attributed to the adiabatic component of torque arising from interaction between DW and spin-polarized current in the ferromagnetic layer hitherto seen in magnetic semiconductor.[8] Another important result concerns the reduced energy barrier to H-driven DW creep in Ta/CoFeB/MgO system as compared to other metallic systems which is an advantageous prospect for DW-based memory devices.[5,6] In Sec. IV, we focus on the underlying factors governing H- and I-induced DW creep motion in the Ta/CoFeB/MgO system.

IV. UNDERLYING FACTORS GOVERNING DW CREEP IN Ta/CoFeB/MgO SYSTEM

The effective critical field for DW motion evidenced from H-induced creep is a reflection of energy landscape for magnetization reversal processes governed by the DW motion. Thus, the observation of weak pinning of DW in the present system requires further clarification with respect to its origin. To this end, we compare $\mu_0 H_C^{\mathrm{eff}}$ between μm devices and un-patterned continuous structure. This allows us to measure the contribution of intrinsic (surface roughness, crystallinity and grain boundaries, etc.) and extrinsic (edge roughness, etc.)[15] effects on the critical field, leading to a quantitative understanding of the origin of the effective critical field.

Figures 3(a) and (b) shows H_Z-driven expansions of a bubble domain observed with the MOKE microscope. Figure 3(c) shows the v vs. $\mu_0 H_Z$ curve, where non-linear relation is observed as well. Using the same method with Sec. III, μ is determined to be 0.23 (inset of Fig. 3(d)), which is the same with the μm-wire devices. Interestingly, evaluation of $\mu_0 H_C^{\mathrm{eff}}$ in the continuous films from the scaling curve shown in Fig. 3(d) leads to a value of 6.5×10^2 T, which is comparable to that obtained for μm-wire devices at the same T. This apparent independence of $\mu_0 H_C^{\mathrm{eff}}$ between un-patterned and patterned structures indicates intrinsic origins rather than extrinsic for reduced pinning in our system.

We also perform TEM structural analysis in order to obtain further insight into correlation between the film crystalline structure and $\mu_0 H_C^{\mathrm{eff}}$. Figure 3(e) shows a cross-sectional TEM images of a film with the stack structure of Ta (0.5 nm)/CoFeB (1.2 nm)/MgO (1.5 nm)/Ta (1 nm). Fourier analysis (lack of lattice fringes) from the CoFeB and MgO layers show that they grow as amorphous layers on the Ta underlayer. This is consistent with our previous results on CoFeB/MgO stack structure with Ta capping. Further investigations (not shown) revealed that amorphous nature of CoFeB layer persists even with thicker Ta underlayer (thickness = 5nm) with partial crystallization of MgO layer. Thus, the reduced effective critical field for Ta/CoFeB/MgO system is expected to arise from the reduction in grain boundaries due to amorphous nature of ferromagnetic layer.
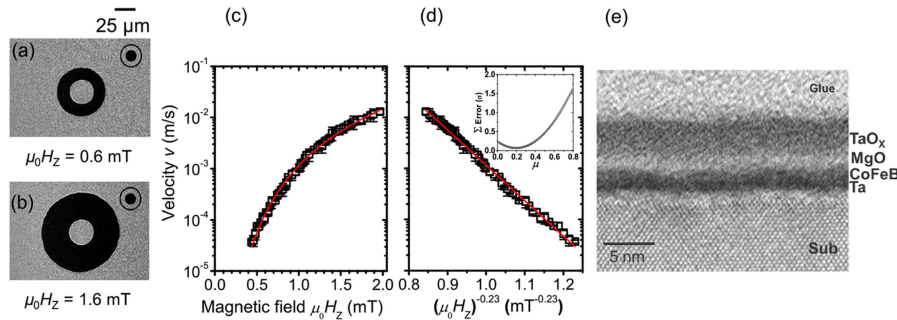

FIG. 3. (a) Differential MOKE image of bubble expansion for $\mu_0 H_Z$ = 0.6 mT. (b) That under $\mu_0 H_Z$ = 1.6 mT. (c) DW velocity v vs. $\mu_0 H_Z$. Black square denotes the experimental data while the red line is the fitting with Eq. (1) and μ = 0.23. (d) Scaling plot of log v vs. $(\mu_0 H_Z)^{-0.23}$. Solid lines indicate the fitting curve. Inset of (d) shows evaluation of μ from minima of standard error. (e) High-resolution cross-sectional TEM image of the stack.

The differences in universality classes for H- and I-induced creep also require further attention concerning mechanism of motion induced by I. It is well known that application of I in heavy metal/ferromagnet/oxide heterostructure results in torque arising from ferromagnetic or heavy metal layer with various symmetries.[17–22] In our previous report, the observed I-induced creep and universality class had been attributed to adiabatic component of spin-transfer torque (STT) arising from interaction between DW and spin-polarized current in the ferromagnetic layer. In systems with broken inversion symmetry, however, a second important factor governing DW motion arises from interfacial Dzyaloshinskii-Moriya interaction (DMI), which also affects the DW dynamics.[20–22] Elucidation of DW configuration determined by DMI along with quantification of torques from various sources in heavy metal/ferromagnet/oxide structure thus enables important insight into dynamics of I-induced creep in metallic systems. To assess presence or absence of DMI in our system, we investigate domain expansion under the application of both in-plane (H_X) and out-of-plane (H_Z) fields in blanket films with identical stack structure. Concentric circular expansion of the bubble domain is modified under an application of H_X if there is finite DMI that favours chiral Néel wall configuration.[23,24] The expansion in Ta/CoFeB/MgO under H_X shows increased expansion along perpendicular direction to applied field as shown in Figs. 4(a) and (b). To quantify the effective field arising from the DMI, we plot DW velocity v_X vs. $\mu_0 H_X$ at a constant $\mu_0 H_Z = 1$ mT, where v_X corresponds to DW velocity along the in-plane field axis. Velocity v_X is calculated as the average of the right moving component for up-down and down-up DW configurations along +x direction. The minima in v vs. $\mu_0 H_X$ curve appears around zero field and shows no appreciable shift within our detection limit of 5 mT unlike the previous studies,[23,24] corresponding to a DMI constant (D) in the range of less than 0.05 mJ/m^2. We have also evaluated DMI constant following the same method as outlined before for the left moving component of DW and the obtained values of D agree with each other within the experimental inaccuracy. We also note that recent experimental results have shown a difference in D determined from bubble domain motion from the one from another technique.[25] Nonetheless, the obtained value of D here is in quantitative agreement with those reported from different measurement techniques for similar systems.[22,26,27] Thus, the shape of bubble expansion together with the obtained value of D supports Bloch DW in our Ta/CoFeB/MgO system.

Next, we discuss the underlying factors determining I-driven motion. The symmetry of torques arising from the current along with DW configuration determines the major driving force to I-induced DW creep. Theoretical and experimental results suggest the existence of four different types of torque which might arise from the current: two arising from spin-orbit torque (SOT) (anti-damping and field-like) and two from STT (adiabatic and non-adiabatic). Here, the Bloch nature of DW dictates that anti-damping and field-like components of SOT are not expected to play a role in I-driven DW motion. The non-adiabatic STT is equivalent to H_Z that can induce steady DW motion. To quantify the net contribution of torques having H_Z symmetry, we investigate I-induced DW creep in the presence of $\mu_0 H_Z$ (= ±0.2 mT). Figure 5 shows the scaling plot of log v vs. $J^{-\mu}$ with $\mu = 0.39$, indicating
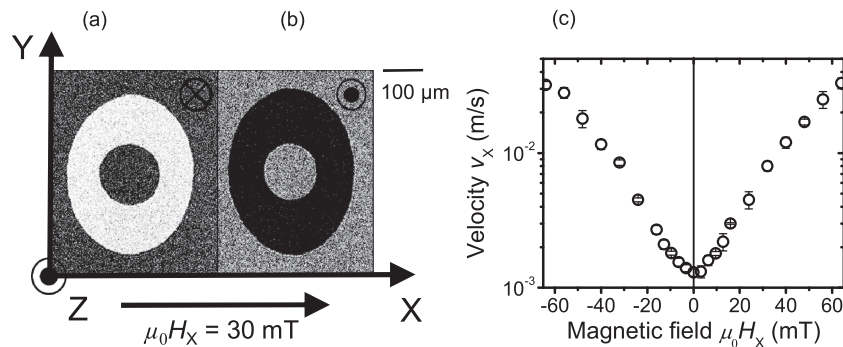

FIG. 4. (a) MOKE images of DW displacement under constant out-of-plane field $\mu_0 H_Z = 1$ mT with $\mu_0 H_X = 30$ mT for upward bubble domain. (b) That for downward bubble domain. (c) v vs. $\mu_0 H_X$ for a constant $\mu_0 H_Z = 1$ mT.
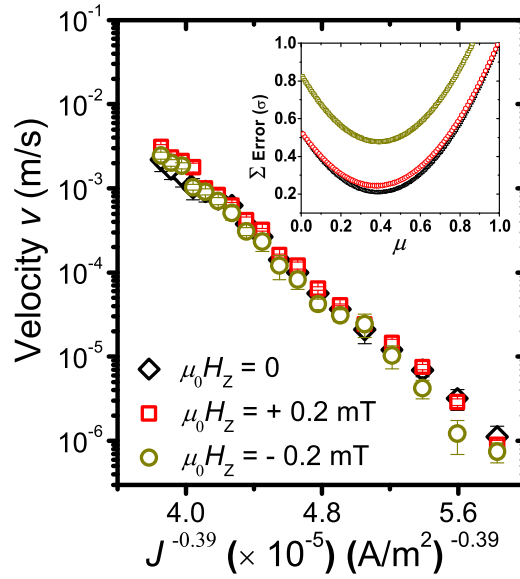
FIG. 5. Scaling plot of current-driven DW creep, log v vs. $J^{-0.39}$, under the application of out-of-plane magnetic field $\mu_0 H_Z$ = 0, ±0.2 mT. The inset shows the evaluation of creep exponent μ for each of the three cases.

insensitivity of I-induced creep to H_Z. This in turn indicates that non-adiabatic STT has minuscule contribution to DW motion. We also note that calculations concerning effective field generated from the non-adiabatic STT using experimental parameters and non-adiabatic coefficient $\beta \sim$ Gilbert damping constant $\alpha \sim 0.01$ indicate that the effective field at the applied maximum J of 2×10^{11} A/m^2 amounts ~ 0.03 mT. This field is much smaller in comparison to H_Z required to drive DWs in the measured velocity range. Thus, Bloch DW configuration in Ta/CoFeB/MgO and miniscule contribution of non-adiabatic STT enable the DW motion dominantly driven by the adiabatic STT, manifesting into the observed universality class for I-driven creep. It is to be mentioned in this regard that previous investigations on fast I-induced DW motion, supported by micromagnetic simulations, have also shown predominance of adiabatic STT on a similar system.[28]

V. SUMMARY

In this article, we review the experimental determination of universality classes for H- and I-driven DW creep in Ta/CoFeB/MgO system and discuss the underlying factors for the results. H-induced DW creep motion in this system shows exceptionally small energy barrier to DW motion in both continuous films and μm-wide devices. This is mainly due to the amorphous nature of ferromagnetic layer resulting in reduced pinning at grain boundaries. We also elaborate underlying factors to I-induced DW creep enabling observation of different universality classes for H- and I-driven DW creep previously unexplored in metallic systems. We show that Bloch DW configuration in this system along with miniscule contribution arising from SOT and non-adiabatic STT enables dominant contribution of the adiabatic STT on the DW creep in the structure with ultrathin Ta underlayer. The present results are expected to provide deeper understanding concerning contribution of different factors for H- and I-induced DW creep.

ACKNOWLEDGMENTS

[1] G. Blatter, M. V. Feigel'man, V. B Geshkenbein, A. I. Larkin, and M. N. Vinokur, Rev. Mod. Phys. **66**, 1125 (1994).

[2] T. Vicsek, M. Cserzö, and V. K. Horváth, Physica A **167**, 315 (1990).

[3] S. V. Buldyrev, A.-L. Barabási, F. Caserta, S. Havlin, H. E. Stanley, and T. Vicsek, Phys. Rev A **45**, R8313 (1992).

[4] S. Lemerle, J. Ferré, C. Chappert, V. Mathet, T. Giamarchi, and P. Le Doussal, Phys. Rev. Lett. **80**, 849 (1998).

[5] S. S. P. Parkin, M. Hayashi, and L. Thomas, Science **320**, 190 (2008).

[6] S. Fukami, M. Yamanouchi, S. Ikeda, and H. Ohno, IEEE Trans. Magn. **50**, 3401006 (2014).

[7] P. Chauve, T. Giamarchi, and P. Le Doussal, Phys. Rev. B **62**, 6241 (2000).

[8] M. Yamanouchi, J. Ieda, F. Matsukura, S. E. Barnes, S. Maekawa, and H. Ohno, Science **317**, 5845 (2007).

[9] J. Kim, K. J. Kim, and S. B. Choe, IEEE Trans. Magn. **45**, 3909 (2009).

[10] A. Kanda, A. Suzuki, F. Matsukura, and H. Ohno, Appl. Phys. Lett. **97**, 032504 (2010).

[11] J.-C. Lee, K.-J. Kim, J. Ryu, K.-W. Moong, S.-J. Yun, G.-H. Gim, K.-S. Lee, K.-H. Shin, H.-W. Lee, and S.-B. Choe, Phys. Rev. Lett. **107**, 067201 (2011).

[12] S. DuttaGupta, S. Fukami, C. Zhang, H. Sato, F. Matsukura, and H. Ohno, Nat. Phys. **12**, 333 (2016).

[13] L. Lari, S. Lea, C. Feeser, B. W. Wessels, and V. K. Lazarov, J. Appl. Phys. **111**, 07C311 (2012).

[14] S. Ikeda, K. Miura, H. Yamamoto, K. Mizunuma, H. D. Gan, M. Endo, S. Kanai, J. Hayakawa, F. Matsukura, and H. Ohno, Nat. Mater. **9**, 721 (2010).

[15] F. Cayssol, D. Ravelosona, C. Chappert, J. Ferré, and J. P. Jamet, Phys. Rev. Lett. **92**, 10 (2004).

[16] R. Lavrijsen, M. A. Verheijen, B. Barcones, J. T. Kohlhepp, H. J. M. Swagten, and B. Koopmans, Appl. Phys. Lett. **98**, 132502 (2011).

[17] L. Berger, J. Appl. Phys. **55**, 1954 (1984).

[18] A. Thiaville, Y. Nakatani, J. Miltat, and Y. Suzuki, Europhys. Lett. **69**, 990 (2005).

[19] T. Koyama, D. Chiba, K. Ueda, K. Kondou, H. Tanigawa, S. Fukami, T. Suzuki, N. Ohshima, N. Ishiwata, Y. Nakatani, K. Kobayashi, and T. Ono, Nat. Mater. **10**, 194 (2011).

[20] S. Emori, U. Bauer, S.-M. Ahn, E. Martinez, and G. S. D. Beach, Nat. Mater. **12**, 611 (2013).

[21] K.-S. Ryu, L. Thomas, S.-H. Yuang, and S. S. P. Parkin, Nat. Nanotech. **8**, 527 (2013).

[22] J. Torrejon, J. Kim, J. Sinha, S. Mitani, M. Hayashi, M. Yamanouchi, and H. Ohno, Nat. Commun. **5**, 4655 (2014).

[23] S.-G. Je, D.-H. Kim, S.-C. Yoo, B.-C. Min, K.-J. Lee, and S.-B. Choe, Phys. Rev. B **88**, 214401 (2013).

[24] D.-Y. Kim, D.-H. Kim, Jo. Moon, and S.-B. Choe, Appl. Phys. Lett **106**, 262403 (2015).

[25] R. Soucaille, M. Belmeguenai, J. Torrejon, J.-V. Kim, T. Devolder, Y. Roussigné, S.-M. Chérif, A. A. Stashkevich, M. Hayashi, and J.-P. Adam, Phys. Rev. B **94**, 104431 (2016).

[26] J.-P. Tetienne, T. Hingant, L. J. Martínez, S. Rohart, A. Thiaville, L. Herrera Diez, K. Garcia, J.-P. Adam, J.-V. Kim, J.-F. Roch, I. M. Miron, G. Gaudin, L. Vila, B. Ocker, D. Ravelosona, and V. Jacques, Nat. Commun. **6**, 6733 (2015).

[27] R. Lo Conte, E. Martinez, A. Hrabec, A. Lamperti, T. Schulz, L. Nasi, L. Lazzarini, R. Mantovan, F. Maccherozzi, S. S. Dhesi, B. Ocker, C. H. Marrows, T. A. Moore, and M. Kläui, Phys. Rev. B **91**, 014433 (2015).

[28] S. Fukami, T. Suzuki, Y. Nakatani, N. Ishiwata, M. Yamanouchi, S. Ikeda, N. Kasai, and H. Ohno, Appl. Phys. Lett. **98**, 082504 (2011).